MMC based SST

Fernando Briz, Mario López, Alberto Rodríguez, Alberto Zapico, Manuel Arias, David Díaz-Reigosa
Department of Electrical Engineering, Universidad de Oviedo, Spain
fernando@isa.uniovi.es

***Abstract* — The Modular Multilevel Converter (MMC) is a type of DC-AC electronic power converter suitable for HVDC applications, thanks to its modularity and to the symmetrical design of the cells. Cells in conventional MMCs use a capacitor in the DC link, meaning that the net power balance of the cell needs to be equal to zero. It is possible however to modify the cells of the MMC to provide the capability to transfer (inject or drain) power. The use of such cells opens several new functionalities and uses for the MMC. Cells with power transfer capability can be used to connect the medium/high voltage DC and AC ports intrinsic to the MMC, with low voltage DC/AC ports, the power transfer among ports being realized at the cell level. This results in multiport power converters, potential applications including solid state transformers (SST). This paper analyzes the design and control of multiport power converters based on MMC topologies, including their use as a SST. Topologies, control strategies and implementation issues will be covered.**

Keywords— Modular Multilevel Converter, MMC, Multiport Power Converters, Medium Frequency Transformer, Solid State Transformer, SST

I. INTRODUCTION

Transformers are key elements in power distribution systems. Classical transformers are a relatively cheap, reliable and well established technology. However, they suffer from several limitations, including low power density (large weight /volume for a certain power) and increased losses at light load. Also, they have an increased sensitivity to harmonics and imbalances.

Solid state transformers (SSTs), also called smart transformers, are an alternative to classical transformers. SSTs use fast-switching power devices to reduce significantly the volume/weight need for the core material. Moreover, SSTs can provide additional functionalities like harmonics, reactive power and imbalances compensation. Consequently, comparison of classical transformer and SST solutions cannot be performed only in terms of price and robustness, additional functionalities provided by SST also need to be considered.

Several topologies have been proposed for the practical realization of the SST [1]-[3]. Criteria for the classification of the existing solutions can include the number of stages (transformations of the electric power format), or whether the power flow can be unidirectional or bidirectional. In all the cases, the SST should connect two AC (normally three-phase) systems and provide galvanic isolation.

This work was supported in part by the Research, Technological Development and Innovation Programs of the Spanish Ministries of Science and Innovation and of Economy and Competitiveness, under grants MICINN- 10-CSD2009-00046 and ENE2013-48727-C2-1-R, and by the European Commission FP7 Large Project NMP3-LA-2013-604057, under grant UE-14-SPEED-604057

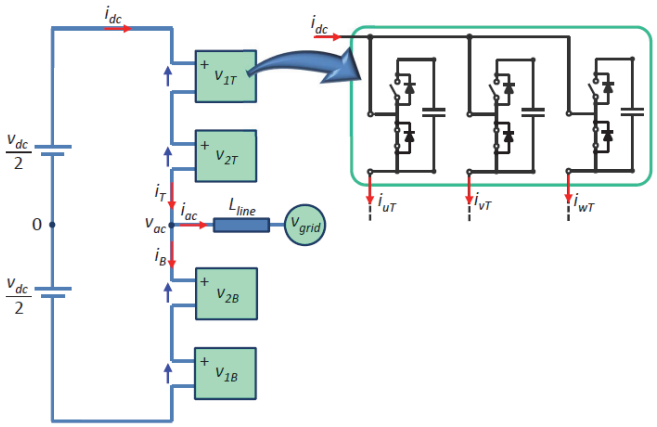

Fig. 1.- Left - Schematic representation of a conventional MMC, with the cells consisting of a half bridge For the sake of clarity, the arm inductances are not shown. Right – Cells using half-bridges for the case of a three-phase MMC.

The Modular Multilevel Converter is a DC/AC electronic power converter that was proposed one decade ago [4]-[6]. The AC port of the MMC can be single-phase or three-phase. All the analysis and discussion in this paper assumes a three-phase AC system. The MMC owns several appealing properties of other modular topologies. Its structure based on simple cells provides scalability, which is key to achieve high voltage levels using relatively low voltage power devices. Losses are significantly reduced due to the low switching frequencies of the individual cells. Also, its modularity results in good output voltage wave shapes, enabling the reduction of the filters as well as of the voltage stress in the power devices [4]-[6]. A distinguishing characteristic of the MMC is that while it provides a high voltage DC link, no bulk DC capacitor is needed. The energy storage is distributed at the cells capacitors. This is advantageous for safety and reliability reasons [7].

Fig. 1 shows the schematic representation of a three-phase MMC. The physical cells forming each arm of the power converter typically consist of a half bridge and a capacitor. Therefore, each cell in Fig. 1-left physically corresponds to three individual cells (Fig. 1-right). Control and modulation strategies developed for MMC are aimed to balance the power transfer between the AC and DC ports, which is done controlling the circulating current [8]-[10], as well as to balance the cell capacitor voltages [10]-[12].

Because the cells of the MMC have a limited energy storage capability, the net power balance for each cell is zero (neglecting losses), the power at the AC and DC sides of the MMC being therefore equal to each other. It is possible to modify the MMC to transfer power at the cell level. This would provide the MMC new potential capabilities, including distributed storage [13]-[15]; integration of distributed energy

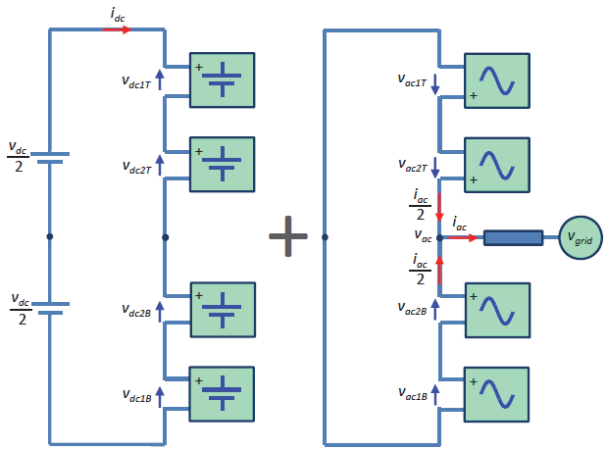

Fig. 2.- DC (left) and AC (right) sub-circuits of the MMC.

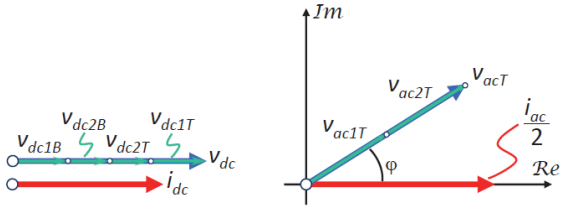

Fig. 3.- DC (left) and AC (right) voltages and currents. Only AC variables for the top arm are shown, they are the same for the bottom arm (see Fig. 2).

resources (DER) at the cell level [16]-[18]; multiport power converters [19]. It is also possible to combine the medium/high voltage DC and AC ports of the MMC with low voltage DC and AC ports. Furthermore, multiport power converters based on the MMC topologies could provide the desired functionalities of the SST, i.e. connection of two AC systems providing galvanic isolation and full control of the power flow, but enhanced with the availability of a high voltage DC link, which is intrinsic to the MMC. However, such modification involves changes both in the cells design as well as in the control strategy [19].

This paper analyzes the design, operation and control of MMCs modified to operate as multiport power converters, including SST. The paper is organized as follows. The model of the conventional MMC is presented in Section II. Design and operation of cells with power transfer capability is discussed in Section III. Multiport power converters based on the MMC, including SSTs, are discussed in Section IV. Control strategies are discussed in Section V. Simulation and experimental results are presented in section VI and VII respectively. Section VIII summarizes the conclusions.

II. Model and Operation of the MMC

The MMC realizes a bidirectional DC-AC power conversion (see Fig. 1). For the discussion following, complex vector notation will be used to represent the AC variables. The voltage and current vectors in the AC port of the MMC are defined by (1) and (2). The resulting top and bottom arm currents are shown in (3), the circulating current i_c being (4), whose DC component is equal to the DC current. Harmonics of the circulating current used e.g. to reduce the oscillations of the cell capacitor voltage [11],[10],[20], are not considered in the analysis following.

$$i_{ac} = \frac{2}{3}\left(i_u + i_v\, e^{j2\pi/3} + i_w\, e^{j4\pi/3}\right) \quad (1)$$

$$v_{ac} = \frac{2}{3}\left(v_u + v_v\, e^{j2\pi/3} + v_w\, e^{j4\pi/3}\right) \quad (2)$$

$$i_T = i_{dc} + \frac{i_{ac}}{2}\ ;\ i_B = i_{dc} - \frac{i_{ac}}{2} \quad (3)$$

$$i_c = \frac{i_T + i_B}{2} = i_{dc} \quad (4)$$

Due to the limited energy storage capability of the cells, the power in the DC port of the MMC has to be equal to the active power in the AC port (5), with * standing for complex conjugate.

$$P_{dc} = v_{dc}\, i_{dc} = P_{ac} = Re\,(v_{ac}\, i_{ac}^*) \quad (5)$$

It is useful to separate the MMC in Fig. 1 into its DC and AC sub-circuits, as shown in Fig. 2. A MMC with two cells per arm (N=2), i.e. Four cells per phase, will be considered as an example for the discussion following. If the MMC is perfectly balanced (identical cells, identical operating point), the cell DC and AC voltages are (6) and (7) respectively, the overall cell voltage being (8). Since the upper and lower arms are connected in parallel, the overall AC voltage needs to be equal to v_{ac}, (see Fig. 2-right). Consequently, the AC current splits equally between the upper and lower arms, all the cells having the same DC and AC powers (9) and (10). It is noted that for the sake of simplicity, the voltage drop in the arm inductor has been neglected in the preceding discussion.

$$v_{dc1T} = v_{dc2T} = v_{dc1B} = v_{dc2B} = \frac{v_{dc}}{2N} = \frac{v_{dc}}{4} \quad (6)$$

$$v_{ac1T} = v_{ac2T} = v_{ac1B} = v_{ac2B} = \frac{v_{ac}}{N} = \frac{v_{ac}}{2} \quad (7)$$

$$v_{nX} = v_{acnX} + v_{dcnX} \quad \text{with } n = 1, 2 \text{ and } X = T, B \quad (8)$$

$$P_{dcnT} = P_{dcnB} = \frac{v_{dc}}{2N}\, i_{dc} = \frac{v_{dc}}{4}\, i_{dc} \qquad ; n = 1, 2 \quad (9)$$

$$P_{acnT} = P_{acnB} = Re\left(\frac{v_{acT}}{N}\ \frac{i_{ac}^*}{2}\right) = Re\left(\frac{v_{acT}}{2}\ \frac{i_{ac}^*}{2}\right) ; n = 1, 2 \quad (10)$$

Fig. 3 graphically shows the DC and AC voltages for the MMC in Fig. 1 and 2. For the AC complex vectors, the real axis real is defined to be aligned with the AC current, φ being the angle between the AC current and voltage vectors. If the voltage at the DC side of the MMC v_{dc} is maintained constant, the MMC control will adjust the DC current i_{dc} to balance the power between the DC and AC ports (5). In addition, the cell capacitor voltages must be kept at their target value. This is done by the balancing algorithms [8],[10],[11].

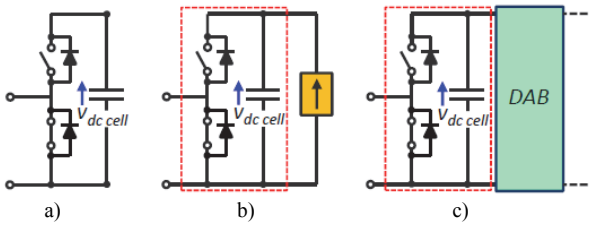

Fig. 4. a) Conventional cell with a capacitor in the DC link; b) cell with power transfer capability using a current source; c) cell using a DAB.

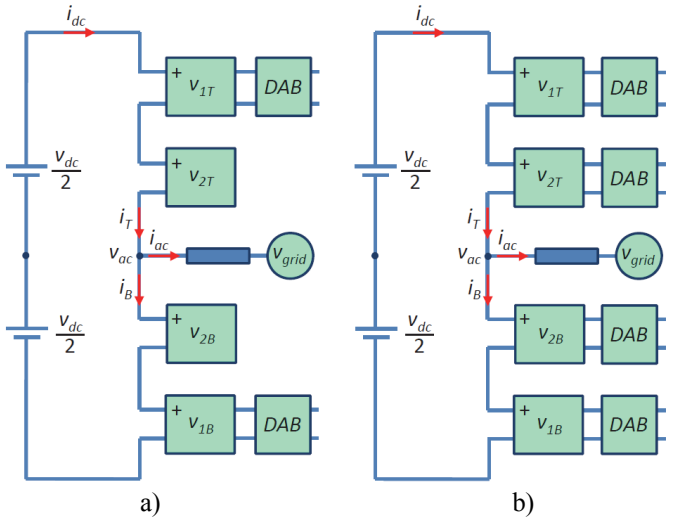

Fig.5.- MMC including cells with power transfer capability. a) MMC in which the same number of cells in the top and bottom arms transfer power; b) MMC in which all the cells transfer power.

III. Cells with Power Transfer Capability

Standard MMC cells have a capacitor in their DC link (see Fig. 1 and Fig. 4a), meaning that the net power balance has to be equal to zero. However, it is possible to provide the MMCs the capability to transfer power at the cell level [19]. Assumed that the cells are controlled to have a constant capacitor voltage of $v_{dc\ cell}$, transferring power to the standard cell design in Fig. 4a can be modeled as a current source connected in parallel to the cell capacitor, as shown in Fig. 4b. In a practical implementation, voltage isolation between the cell capacitor and the power source might be needed, a current controlled dual active bridge (DAB) can be used for this purpose (Fig. 4c) [2],[19],[21],[22].

If one or more cells transfer power, the resulting MMC power balance equation is (11), where P_{cell} is the power transferred by each cell and M is the number of cells transferring power. It is assumed that all the cells transfer a similar amount of power.

$$P_{dc} + MP_{cell} = P_{ac} \tag{11}$$

Two major cases can be considered for the case in which there are cells with the capability to transfer power: 1) only some cells of the MMC have that capability, and 2) all the cells of the MMC have this capability. These two cases are schematically represented in Fig. 5a and Fig. 5b respectively.

The case shown in Fig. 5a in which only some cells transfer power, will result in asymmetries in the mode of operation of the cells. Consequently, cells in the same arm will have different AC and/or DC voltages, depending on whether they transfer power or not. This produces significant differences with respect to the normal operation of the MMC, where all the cells have (ideally) the same DC and AC voltages (switching harmonics neglected). Modification of the control strategy can be required in this case, as conventional control strategies assume that all the cells operate identically. Furthermore, the fact that not all the cells inject power, will place limitations on how the power injected by the cells can be split between the AC and DC ports of the MMC. Detailed discussion of this can be found in [19].

In the case shown in Fig. 5b, all the cells operate in the same working conditions, provided that they transfer a similar amount of power. Due to this, control of the MMC is significantly simpler compared to the case in Fig. 5a. This case is analyzed in detail in the next sections, as will be the base of the proposed multiport power converter topology.

IV. Multiport Topologies Based on the MMC

Providing the cells of the MMC the capability to transfer power opens several opportunities to realize multiport power converters. Examples of these are shown in Fig. 6a-c. In all the configurations shown in this figure, the left-side of the power converter corresponds to an MMC AC and DC ports, and will be considered as the high-voltage (HV) side. For simplicity, the MMCs in the figure use two cells per arm (N=2). However, all the discussion following can be extended to any value of N without any loss of generality. In all the cases, the isolation between the high voltage (HV) and low voltage (LV) AC ports is realized by DABs. It is also observed that in all the implementations, each cell of the MMC is connected to a DAB, meaning that the modularity of the MMC is extended to the isolation stage formed by the DABs. The right side of the power converter in Fig. 6a-c will be considered as the LV side. It is seen that the differences among the topologies shown in Fig. 6 only affect to the LV side.

The configuration shown in Fig. 6a corresponds to two MMC connected through the cells capacitors and the DABs. It provides two AC ports and two DC ports (HV and LV), with the same number of voltage levels in both AC ports. Since the number of cells is the same in both sides, the transformation HV-to-LV between the primary and the secondary has to be realized by the DABs. Consequently, the DAB are not symmetrical. The left (HV) side of the power converter will require high voltage-low current power devices, while the cells in the right (LV) side would use low voltage-high current power devices.

The configuration shown in Fig. 6b also corresponds to two MMC connected through the cells capacitors and the DABs. Therefore, it also provides two AC ports and two DC ports. However, in this case the DABs in each arm of the HV side are serialized, while there is some level of parallelization in the LV side. As a consequence, the number of cells (and thus the number of voltage levels) in the HV and LV sides are different. With this configuration, the transformation HV-to-LV

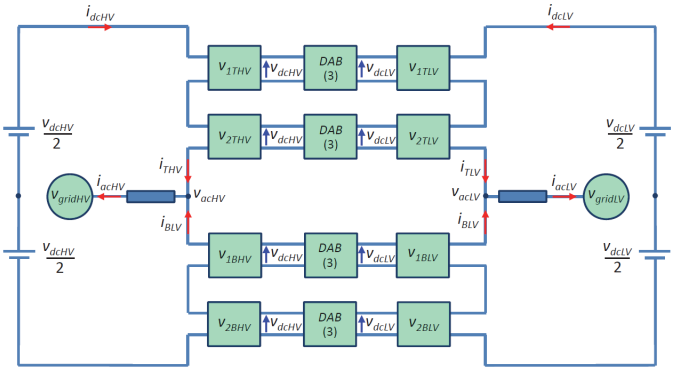

a) Cell-to-cell connected MMCs with symmetric primary and secondary (serialized input-serialized output).

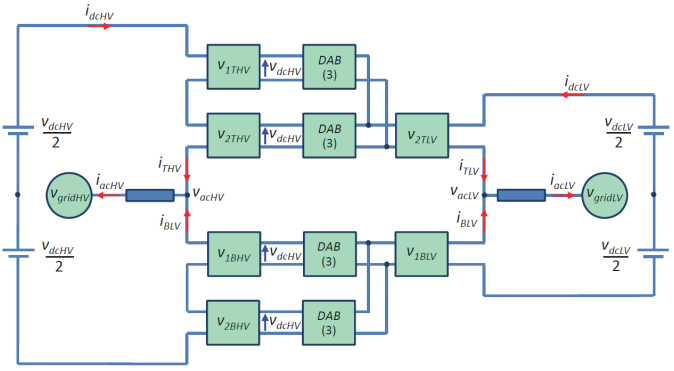

b) Cell-to-cell connected MMCs with serialized input-parallelized output.

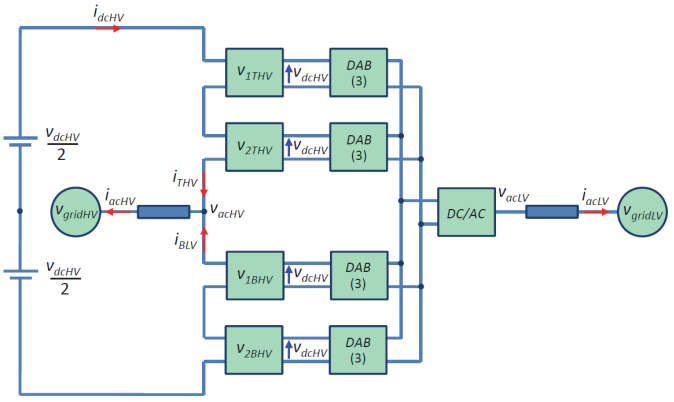

c) Multiport power converter with and MMC in the HV side and a conventional AC/DC power converter in the LV side.

Fig. 6. Different configurations of MMC based multiport power converters.

between the primary and the secondary does not have to be realized only by the DABs, but can also be achieved by the effect of the serialization/ parallelization of the DBAs in the HV/LV sides respectively. This means that power devices with the same or close voltage ratings can be used now for the HV and LV sides.

Finally, in the configuration shown in Fig. 6c, all the DABs in each leg are connected in parallel in the LV side. As a consequence, a conventional DC/AC power converter can be used now (e.g. Two level or multilevel NPC, FC, …). In this configuration, the transformation HV-to-LV between the primary and the secondary can be entirely obtained by the effect of the serialization/parallelization of the DBAs in the

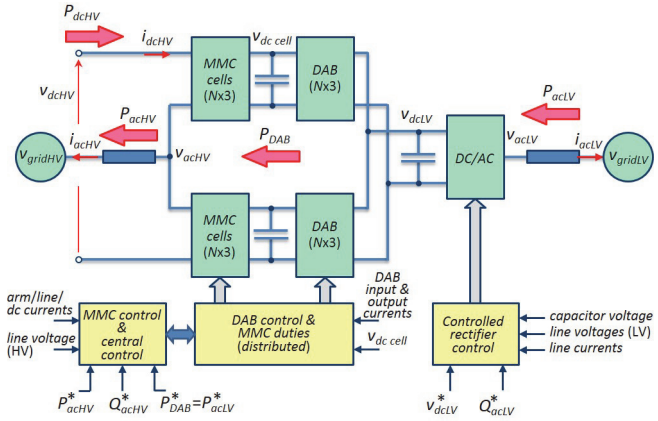

Fig. 7. Schematic representation of the control of the multiport power converter. Variables with "*" indicate commanded values. Variables without "*" indicate measured signals needed used by the control.

HV/LV sides. Thus, the DABs could now be symmetric, with a ratio 1:1 between the primary and the secondary. This would allow to use the same power devices in both sides.

It is important to note that Fig. 6c shows explicitly three ports: HV-DC, HV-AC, and LV-AC. Though a LV-DC port also exists, it is not shown in the figure, as it will not be considered in the discussion following. This means that the power transferred by the DABs needs to be equal to the active power of the AC port in the LV side (losses neglected). Control and behavior of the topology shown in Fig. 6c is discussed in the following sections.

V. Control Strategies

This section addresses the control for the multiport power converter shown in Fig. 6c. The power balance equation is given by (12). If losses are neglected, the power transferred by the DAB will be equal to the active power of the DC/AC power converter in the LV side (13).

$$P_{acLV} + P_{dc} = P_{acHV} \tag{12}$$

$$P_{DAB} = P_{acLV} \tag{13}$$

In the discussion following, it is assumed that the power transferred by the DAB (and consequently P_{acLV}) and the active power in the HV AC port P_{acHV} are the commanded values. Consequently, the power in the DC port of the MMC P_{dc} needs to be adapted by the MMC control to realize the power balance. This is done by controlling the circulating current.

Fig. 7 shows a potential implementation of the control. It is seen to consist of three major blocks:

- MMC control
- DAB control
- Controlled rectifier (DC/AC converter in the LV side) control

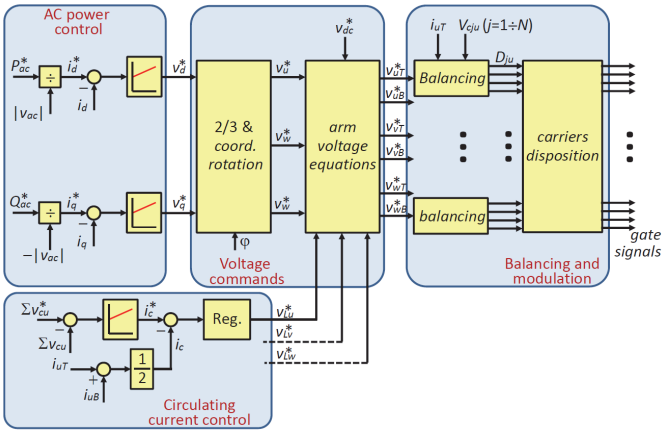

Fig. 8. Control of the MMC.

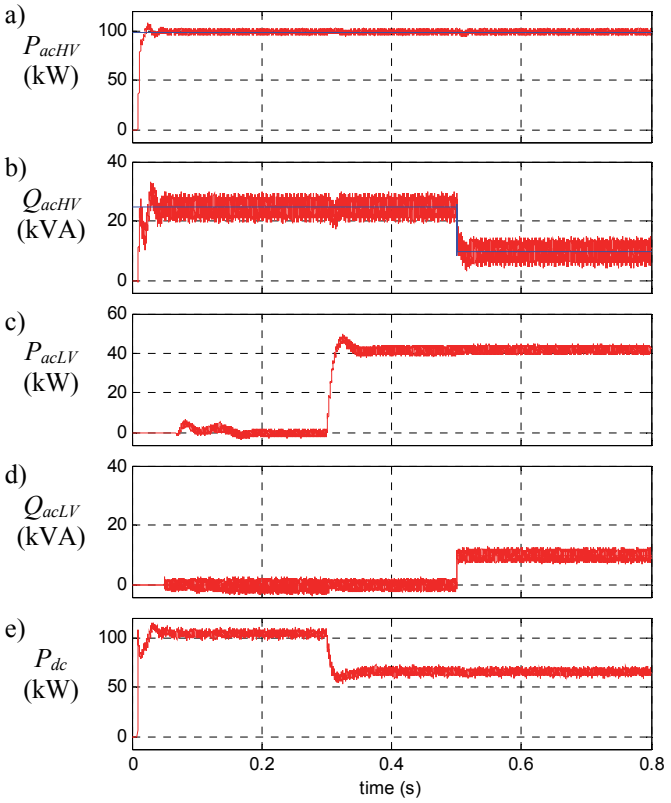

Fig. 9. Simulation results. Active and reactive power at the different stages of the power converter. a) active power in the HV AC side, b) reactive power in the HV AC side, c) active power in the LV AC side, d) reactive power in the LV AC side, e) power in the DC link of the MMC.

MMC control: The MMC control implements the normal functionalities for this type of power converter [10]. Multiple control objectives need to be satisfied simultaneously, a potential control strategy being shown in Fig. 8:

- d and q-axis current references for the HV AC side are obtained from the active and reactive power commands. Synchronous PI current regulators are used to obtain the required d and q-axis voltage commands.
- In order to guarantee the power balance between the DC and AC ports, the energy stored in the arm capacitors –and therefore the capacitors voltage– must remain constant. The circulating current command is obtained from the errors in the overall cell capacitors voltage, a PI controller being used for this purpose. The voltage applied to the arm inductors is used to control the circulating current.
- Once the voltage commands for the upper and lower arms are obtained, balancing of the cell capacitors voltages is required. A sorting algorithm is implemented in Fig. 8 [4]-[6]. In this strategy, the cells to be inserted are selected based on the capacitors voltage needs and the direction of the arm currents.
- Finally, gate signals are obtained by means of a level-shifted PWM modulation.

In the prototype under construction, the control of the MMC is distributed between a master control unit based on a Zynq SoC (System on a chip) by Xilinx, and several slave control units based on FPGAs. Details on the implementation of the control can be found in [23].

DAB control: The DABs operate as current sources. Each DAB includes a low cost FPGA, their control being therefore distributed. It is noted that the DABs do not control their input and output voltages. This is done by the MMC through the control of the cell capacitors $v_{dc\ cell}$, and by the controlled rectifier, which controls the capacitor voltage in the low voltage DC link $v_{dc\ LV}$. It is also noted that though the DABs receive a current command, this directly corresponds to a power command, provided that the input and output voltages are maintained at their target values. The current commands are the same for all the DABs, they are sent by the central control via optic fiber.

AC/DC converter control: The AC/DC power converter in the low voltage side is controlled as a conventional controlled rectifier. The commanded values are the DC link voltage and the reactive power. The active power is internally controlled to maintain the DC link capacitor $v_{dc\ LV}$ at its target value. The control is implemented on a DSP. The reactive power command is received from the central control.

The signals that need to be measured by each control block are also shown in Fig. 7. It is noted that for the MMC control, the DC current, AC currents and arm currents can be needed for different control purposes. Since these currents are not independent variables, there are different options for the placement of the current sensors. Measuring the top and bottom arm currents is sufficient in principle to estimate the other currents. However, redundant sensors are often used to improve the accuracy and reliability.

VI. Simulation Results

The operation of power converter topology shown in Fig 7 has been simulated using Matlab/Simulink. Fig. 9 shows the behavior of the system in different modes of operation. The MMC is enabled at t=10 ms, with, the active and reactive power commands being 100 kW (Fig. 9a) and 25 kVAr (Fig. 9b) respectively. Initially the DABs are not transferring power. Therefore, the power in the DC link of the MMC (Fig. 9e) matches the AC power plus the converter losses. At t=70 ms

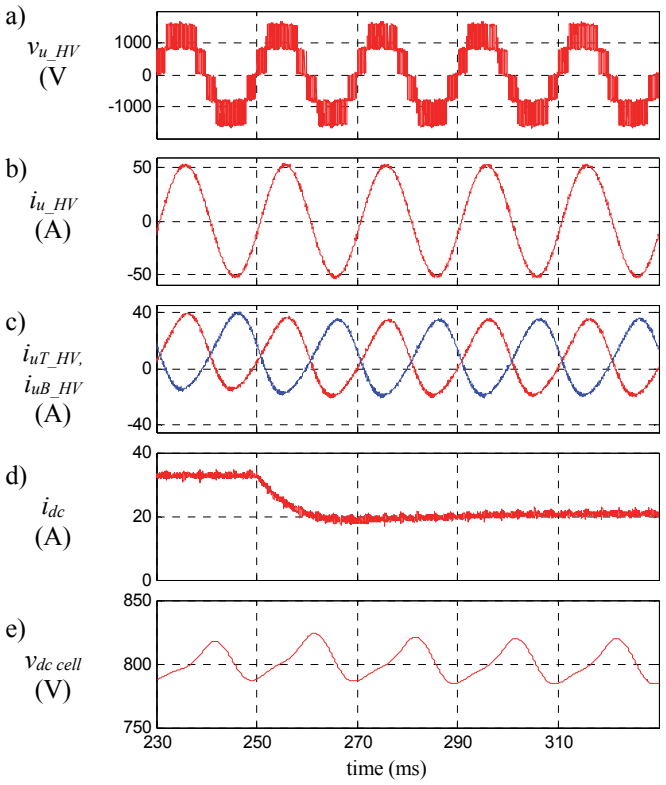

Fig. 10. Simulation results. Voltages and currents at different stages of the MMC. a) phase *u* voltage, b) phase *u* currant, c) currents in the top and bottom arms of phase *u*, d) dc current, e) capacitor voltage in one cell of the MMC.

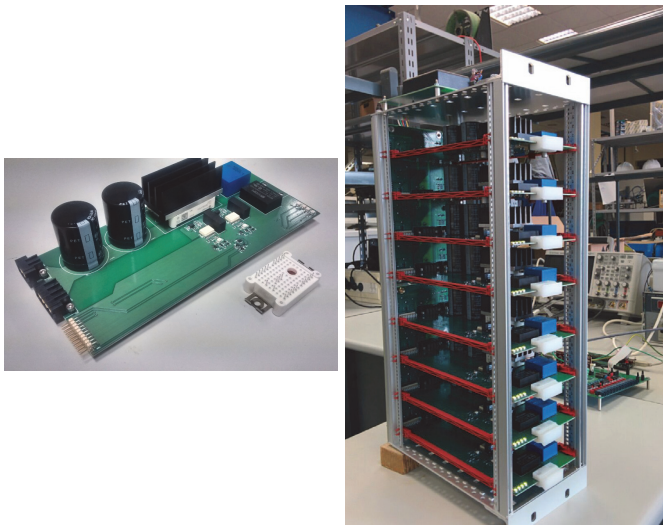

Fig. 11. Experimental prototype. Left – MMC cell.; right – MMC leg consisting of eight cells, inserted in the rack.

the controlled rectifier in the LV side of Fig. 7 is enabled (Fig. 9c). However, initially it will not transfer active power, since the DABs are not transferring power either. The reactive power command for the controlled rectifier in the LV side is also set initially to zero (Fig. 9d). In t=0.3 s, the DABs are commanded to transfer a total amount of 40 kW. This power is supplied by the controlled rectifier in the LV side (Fig. 9d).

TABLE I: EXPERIMENTAL SETUP

MMC	Power switches	600V/23A
	Cell capacitor / Arm inductance	2000uF / 1mH
	Cell voltage / DC bus voltage	80 V / 320 V
	Sampling frequency	5 kHz
DAB	Input / output voltage	12 V / 50 V
	Switching frequency	100 kHz
	Turn ratio / Leakage inductance of the transformer	N=4 / L_k=5uH

It is also observed from Fig. 9e that the power supplied by the DC bus of the MMC is decreased in the same amount, as needed to maintain the power balance. As discussed in the preceding section, only the AC active power in the HV side of the MMC and the power transferred by the DABs are commanded. The active power for the controlled rectifier and the power in the DC link of the MMC are adapted by the corresponding controls (see Fig. 7) to maintain the power balance. As already mentioned, the reactive power in the HV side (Fig. 9b) and LV side (Fig. 9d) are controlled independently, the only restriction coming from the current ratings of the power devices and passive elements of each power converter.

Fig. 10 shows a closer view of the voltages and currents at different stages of the MMC during the transient in Fig. 9 occurring at t=0.3 s. It is observed that the phase voltages and currents in the AC port of the MMC do not change, as the AC power in the HV side remains constant during the transient. Injection of power from the LV side through the controller rectifier and the DABs results in a decrease of the DC current of the MMC (Fig. 10d), and consequently of the DC component of the top and bottom arm currents of the MMC (Fig. 10c). Finally, Fig. 10e shows the capacitor voltage of one cell of the MMC. The ripple due to the oscillations of the phase power of the MMC are readily visible. The balancing algorithm implemented in the MMC control maintains these oscillations within admissible limits, not having any adverse effect on the MMC response.

VII. EXPERIMENTAL RESULTS

The experimental setup needed for the implementation of the proposed concepts is under construction. Preliminary results are shown in this section.

The MMC prototype consists of eight cells (N=4). Fig. 11-left shows one cell of the MMC. Fig. 11-right shows one leg of the MMC. The cells are seen to be inserted in a rack, the connectors both for the control signals as well for the power (cell DC link) being located in a back-plane.

Currently, one leg of the MMC and two DAB have been built and are operative. This means that a topology of the type shown in Fig. 5a, but for the case of single phase MMC, can be experimentally tested. The other two legs of the MMC have also been built. However, development and construction of the final version of the DABs is not complete yet. They are expected to be operative in a few months. The implementation of the control is as described in Section V.

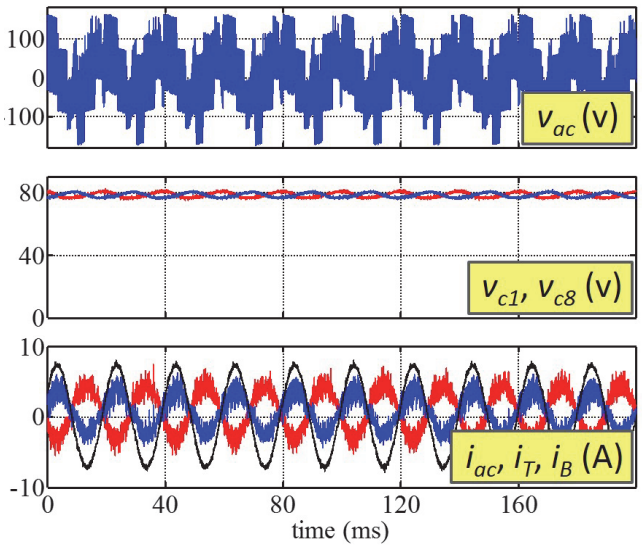

Fig. 12.- Experimental results. Top: v_{ac}; mid: capacitor voltage for cells 1&8, bottom: i_P, i_N and i_{ac} currents.

The details of the MMC and the DABs can be found in Table II. The DABs realize a bidirectional DC/DC conversion. It uses two active full bridges interfaced through a high-frequency transformer, which provides galvanic isolation. Soft-switching operation of all the devices at nominal conditions is possible. Two complementary signals with a 50% duty cycle were used to control each full bridge. The power flow is controlled by varying the phase-shift between these signals. Feedback control with a PI regulator was used to control the current injected to the cell by the DABs [21],[22].

Fig. 12 shows an example of the normal operation of the MMC, i.e. without power transfer.

Fig. 13-left shows the DC component as well as the magnitude and phase of the AC (50 Hz) component of the cells voltage for the top arm, both for the case when the cells do not transfer power (conventional MMC) and when one cell per arm transfers power. Bottom arm behaves similarly, and is not shown. The power transferred by the cells P_{cell} is 20% of the AC power P_{ac}. Fig. 13-right shows the power in the DC and AC sides of the MMC, as well as the power transferred by the cells. The MMC is controlled to maintain constant the power in the AC side, meaning that power transferred by the cells is reflected in the power in the DC side of the converter.

VIII. Conclusions

Multiport power converters based on MMC topologies have been proposed and analyzed in this paper. The proposed concept can connect high voltage and low voltage DC ports and AC ports, providing therefore the functionalities of a solid state transformer. Isolation is provided by DABs through a modular structure. Control strategies have also been discussed. Simulation results as well as preliminary experimental results confirming the viability of the proposed concepts have been provided.

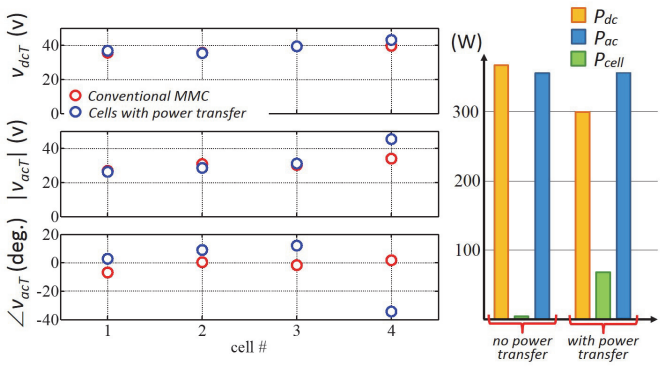

b) $P_{cell} = 0.2\ P_{ac}$

Fig. 13.- Experimental results. Left: DC and AC component of the cell voltage (only results for cells #1 to #4 shown); right: DC, AC and cells power without/with cell power transfer, for two different values of the power transferred by the cells. P_{ac} remains constant when the cells transfer power.

References

[1] Falcones, S.; Xiaolin Mao; Ayyanar, R., "Topology comparison for Solid State Transformer implementation," *Power and Energy Society General Meeting, 2010 IEEE* , vol., no., pp.1,8, 25-29 July 2010

[2] Zhao, T.; Wang, G.; Bhattacharya, S.; Huang, A Q., "Voltage and Power Balance Control for a Cascaded H-Bridge Converter-Based Solid-State Transformer," IEEE Trans. on Power Elect., vol.28, no.4, pp.1523-1532, April 2013.

[3] Zhu Haibin; Li Yaohua; Wang Ping; Li Zixin; Chu Zunfang, "Design of Power Electronic Transformer Based on Modular Multilevel Converter," *Power and Energy Engineering Conference (APPEEC), 2012 Asia-Pacific*, vol., no., pp.1,4, 27-29 March 2012

[4] A. Lesnicar, and R. Marquardt: An Innovative Modular Multilevel Converter Topology Suitable for a Wide Power Range, IEEE PowerTech Conference, Bologna, Italy, June 23-26, 2003.

[5] M. Glinka and R. Marquardt: A New AC/AC Multilevel Converter Family, IEEE Trans. on Industrial Electronics, vol. 52, no. 3, June 2005.

[6] A. Lesnicar, and R. Marquardt: A new modular voltage source inverter topology, EPE 2003, Toulouse, France, September 2-4, 2003.

[7] Rohner, S.; Bernet, S.; Hiller, M.; Sommer, R.; "Analysis and Simulation of a 6 kV, 6 MVA Modular Multilevel Converter," 35th Annual Conf. of IEEE Ind. Elect.. IECON '09., pp. 225-230, 3-5 Nov. 2009.

[8] Hagiwara, M.; Akagi, H.; "Control and Experiment of Pulsewidth-Modulated Modular Multilevel Converters," Power Electronics, IEEE Trans. on, vol.24, no.7, pp.1737-1746, July 2009.

[9] Antonopoulos, A.; Angquist, L.; Nee, H.-P.; "On dynamics and voltage control of the Modular Multilevel Converter," 13th European Conference on Power Elect. and Appl., 2009. EPE '09. pp.1-10, 8-10 Sept. 2009.

[10] Jae-Jung Jung; Hak-Jun Lee; Seung-Ki Sul, "Control strategy for improved dynamic performance of variable-speed drives with the Modular Multilevel Converter," Energy Conversion Congress and Exposition (ECCE), 2013 IEEE, pp.1481-1488, 15-19 Sept. 2013.

[11] Perez, M.A.; Bernet, S.; Rodriguez, J.; Kouro, S.; Lizana, R., "Circuit Topologies, Modeling, Control Schemes, and Applications of Modular Multilevel Converters," *Power Electronics, IEEE Transactions on* , vol.30, no.1, pp.4,17, Jan. 2015

[12] Saeedifard, M.; Iravani, R., "Dynamic Performance of a Modular Multilevel Back-to-Back HVDC System," Power Delivery, IEEE Trans. on, vol.25, no.4, pp.2903-2912, Oct. 2010.

[13] I. Trintis, S. Munk-Nielsen, and R. Teodorescu, "A new modular multilevel converter with integrated energy storage," in Proc. IEEE 37th Annu. Conf. Ind. Electron. Soc., 2011, pp. 1075–1080.

[14] Vasiladiotis, M.; Rufer, A., "Analysis and Control of Modular Multilevel Converters With Integrated Battery Energy Storage," *Power Electronics, IEEE Transactions on* , vol.30, no.1, pp.163,175, Jan. 2015

[15] Vasiladiotis, M.; Rufer, A., "A Modular Multiport Power Electronic Transformer With Integrated Split Battery Energy Storage for Versatile Ultra-Fast EV Charging Stations,"*Industrial Electronics, IEEE Transactions on* , vol.PP, no.99, pp.1,1

[16] M. A. Perez, D. Arancibia, S. Kouro, and J. Rodriguez, "Modular multilevel converter with integrated storage for solar photovoltaic applications," in Proc. IEEE 39th Annu. Conf. Ind. Electron. Soc., 2013, pp. 6993–6998.

[17] B. Alajmi, K. Ahmed, G. P. Adam, S. Finney, and B. Williams, "Modular multilevel inverter with maximum power point tracking for grid connected photovoltaic application," in Proc. IEEE Int. Symp. Ind. Electron., 2011, pp. 2057–2062.

[18] J. Mei, B. Xiao, K. Shen, L. Tolbert, and J. Y. Zheng, "Modular multilevel inverter with new modulation method and its application to photovoltaic grid-connected generator," IEEE Trans. Power Electron., vol. 28, no. 11, pp. 5063–5073, Nov. 2013

[19] Fernando Briz, Mario Lopez, Alberto Zapico, Alberto Rodriguez, David Diaz-Reigosa, "Operation and Control of MMCs Using Cells with Power Transfer Capability," 30th Annual IEEE Applied Power Electronics Conference & Exposition (APEC), 15-19 March 2015, Charlotte, NC, USA

[20] Hagiwara, M.; Hasegawa, I.; Akagi, H., "Start-Up and Low-Speed Operation of an Electric Motor Driven by a Modular Multilevel Cascade Inverter," IEEE Trans. on Ind. Appl., vol.49, no.4, pp.1556,1565, July-Aug. 2013

[21] DeDoncker, R. W.; Divan, R. W.; Kheraluwala, M.H., "A three-phase soft-switched high power-density dc/dc converter for high –power applications". IEEE Trans. on Ind. Appl., vol. 27, p. 63-73. Jan. 1991.

[22] Rodriguez, A.; Vazquez, A.; Lamar, D.G.; Hernando, M.M.; Sebastian, J., "Different Purpose Design Strategies and Techniques to Improve the Performance of a Dual Active Bridge With Phase-Shift Control," IEEE Trans. on Power Elect., vol.30, no.2, pp.790,804, Feb. 2

[23] M. López, A. Rodríguez, E. Blanco, M. Saeed, Á. Martínez, F. Briz, "Design and Implementation of the Control of a MMC Based Solid State Transformer," IEEE International Conference on Industrial Informatics INDIN'15, 22-24 July 2015, Cambridge, UK